

AD-A250 893



ATION PAGE

Form Approved  
OMB No. 0704-0199

2

To average 1 hour per response, including the time for reviewing instructions, searching existing data sources, gathering the collection of information, send comments regarding this burden estimate or any other aspect of this form to Washington Headquarters Services, Directorate for Information Operations and Reports, 1215 Jefferson Avenue, Washington, DC 20540.

1. AGENCY USE ONLY (Leave blank)		2. REPORT DATE 31 Mar 92		3. REPORT TYPE AND DATES COVERED Final Report - 31 Oct 1988 to 30 Sept 1991	
4. TITLE AND SUBTITLE 3-D Analysis and Verification of Fracture Growth Mechanisms in Fiber-Reinforced Ceramic Composites				5. FUNDING NUMBERS AFOSR-89-0005	
6. AUTHOR(S) Prof. M.P. Cleary, Dr. W.D. Keat, Capt. M.C. Larson, F.T. Patterson					
7. PERFORMING ORGANIZATION NAME(S) AND ADDRESS(ES) Massachusetts Institute of Technology 77 Massachusetts Ave. Cambridge, MA 02139				8. PERFORMING ORGANIZATION REPORT NUMBER AFOSR-TR-92 0417	
9. SPONSORING / MONITORING AGENCY NAME(S) AND ADDRESS(ES) Air Force Office of Scientific Research (AFOSR / NA) Building 410 Bolling AFB, DC 20332-6448				10. SPONSORING / MONITORING AGENCY REPORT NUMBER N/A	
11. SUPPLEMENTARY NOTES N/A					
12a. DISTRIBUTION / AVAILABILITY STATEMENT Approved for public release; Distribution unlimited.				12b. DISTRIBUTION CODE N/A	

DTIC  
SELECTE  
MAY 26 1992  
S D

ABSTRACT (Maximum 200 words)

This final report documents a 3-D computational and experimental investigation into the mechanics of toughening a brittle matrix by incorporating long brittle fibers. Computationally, small scale failure mechanisms ahead of a crack are explicitly modeled and merged with a continuum representation of the far field outside the process zone. Particular attention is given to the interfacial decohesion and frictional slipping near the tip of a matrix crack which is impinging upon an inclusion. The surface integral and finite element (SIFEH) method, which employs the principle of superposition to combine the best features of two powerful numerical techniques, provides an extremely flexible and efficient computational platform for modeling linear elastic fractures near material inhomogeneities. Applications to general 3-D fracture growth in multimaterial media demonstrate the capabilities of the computational technique and are also described. The computational simulation is being guided by laboratory experiments. Crack growth observations made on a model (micro-) structure comprising a glass rod embedded in a cement matrix show the toughening mechanisms of crack pinning and crack bridging in operation. In a second experiment, interfacial slip evolution was modeled experimentally for planar bimaterial interfaces. This combined experimental and numerical program is providing insight into optimal combinations of the key parameters (e.g. residual stresses at interface, friction coefficient, strength of fibers) to maximize toughness.

92 5 22 053

14. SUBJECT TERMS Fracture Mechanics; Fiber-Reinforced Composites; Ceramic Composite Materials; Surface-Integral Method;			15. NUMBER OF PAGES	
			16. PRICE CODE	
17. SECURITY CLASSIFICATION OF REPORT UNCLASSIFIED	18. SECURITY CLASSIFICATION OF THIS PAGE UNCLASSIFIED	19. SECURITY CLASSIFICATION OF ABSTRACT UNCLASSIFIED	20. LIMITATION OF ABSTRACT SAR	

92-13728



Air Force Contract No. AFOSR-89-0005

**3-D ANALYSIS AND VERIFICATION OF FRACTURE GROWTH  
MECHANISMS IN FIBER-REINFORCED CERAMIC COMPOSITES**

**Michael P. Cleary, Associate Professor  
Department of Mechanical Engineering  
Massachusetts Institute of Technology  
Cambridge, MA 02139**

31 March 1992

Final Report

Prepared for:  
**Air Force Office of Scientific Research  
Building 410  
Bolling AFB, D.C. 20332**

# **3-D Analysis and Verification of Fracture Growth Mechanisms in Fiber-Reinforced Ceramic Composites**

## Final Report

Michael Cleary, Principal Investigator  
Associate Professor  
M.I.T.

Dr. C.I. Chang, Dr. John Botsis  
Director of Aerospace Science  
AFOSR

## **SUMMARY**

This final report documents a 3-D computational and experimental investigation into the mechanics of toughening a brittle matrix by incorporating long brittle fibers. Computationally, small scale failure mechanisms ahead of a crack are explicitly modeled and merged with a continuum representation of the far field outside the process zone. Particular attention is given to the interfacial decohesion and frictional slipping near the tip of a matrix crack which is impinging upon an inclusion. The surface integral and finite element (SIFEH) method, which employs the principle of superposition to combine the best features of two powerful numerical techniques, provides an extremely flexible and efficient computational platform for modeling linear elastic fractures near material inhomogeneities. Applications to general 3-D fracture growth in multimaterial media demonstrate the capabilities of the computational technique and are also described. The computational simulation is being guided by laboratory experiments. Crack growth observations made on a model (micro-) structure comprising a glass rod embedded in a cement matrix show the toughening mechanisms of crack pinning and crack bridging in operation. In a second experiment, interfacial slip evolution was modeled experimentally for planar bimaterial interfaces. This combined experimental and numerical program is providing insight into optimal combinations of the key parameters (e.g. residual stresses at interface, friction coefficient, strength of fibers) to maximize toughness.

Efforts to further improve the SIFEH method for this application are continuing with the support of a contract extension. A comprehensive research report will be provided at the completion of this investigation.

## INTRODUCTION

The key episode in the fracture of a ceramic matrix/ceramic fiber composite is the interaction that takes place between an advancing crack front and the fiber-matrix interface of individual fibers. A "strong" interface will transmit high crack tip stresses inducing premature fracture of the fibers, while a "weak" interface will blunt the crack tip and allow the fracture to proceed past intact fibers. The 2-D analysis by He and Hutchinson<sup>1</sup> gives the design "rule of thumb" that the fracture toughness of the interface should be less than one-quarter of the toughness of the fiber to promote favorable toughening mechanisms such as bridging and pull-out. However, a completely "weak" interface will not generate the desirable friction tractions to shield the crack tip. An optimum therefore exists with regard to toughness of the material and physical properties, including interfacial bond, toughness, and friction characteristics.

Recent investigations, while providing insight to these toughening mechanisms, are restricted in their applicability by simplifying assumptions whose impact is often difficult to assess. A number of 2-D analyses have been carried out for cracks near sliding and bonding interfaces,<sup>1-3</sup> some of these in the context of fibrous inclusions.<sup>4-8</sup> Axisymmetric models which account for frictional tractions on the interface have also been developed<sup>9,10</sup> for the special case of a single fiber that is completely engulfed by a fracture. Other work has examined crack pinning by bonded cylindrical inclusions.<sup>11,12</sup>

This summary report outlines a combined computational and experimental investigation aimed at providing a complete fracture mechanics analysis of a crack growing near a fiber and interacting with the evolving frictional sliding zone at the interface (see Fig. 1) An innovative numerical scheme, the surface integral and finite element hybrid (SIFEH) method, has been developed to obtain results for cracks near and/or crossing multiple bimaterial interfaces. Extensions are now underway to account for the frictional tractions and curvature of the fiber-matrix interface. In addition, novel experimental tools are being employed to verify the computational solutions.

For	
I	<input checked="" type="checkbox"/>
d	<input type="checkbox"/>
ion	<input type="checkbox"/>

By	
Distribution/	
Availability Codes	
Dist	Avail and/or Special
A-1	



## DESCRIPTION OF COMPUTATIONAL APPROACH

### Modeling Requirements:

Until very recently, the direct numerical modeling of the situation depicted in Figure 1 would have been viewed as impractical. The most common tool available, finite elements, was known to require an extraordinary number of degrees of freedom to capture the stress singularity along the crack periphery, a situation that was made all the more untenable by the need to globally remesh after each time step. Thus an alternate approach was sought.

In formulating the numerical procedure presented here, we have kept in mind that a suitable computational approach should not only possess sufficient generality to address the problem of Figure 1, but it should also meet the following efficiency and accuracy requirements:

*Accurate Stress Intensity Factors:* The difficulty in modeling a fracture lies in being able to accurately represent the singularity in stress along the continuous crack front. The accuracy is usually assessed in terms of the stress intensity factor, which serves both as a measure of the strength of the singularity and as a criterion for crack growth. It is typically desirable to maintain the error in stress intensity factor at less than a few percent because of the error amplification associated with some crack growth laws, especially in metal fatigue.

*Effective Modeling of Crack Propagation:* This is achieved by keeping the total number of degrees of freedom in the problem to a minimum while providing a facility for remeshing the element topology as the crack front advances. The fact that the geometry of Fig. 1 may be viewed as consisting of multiple growing fractures (i.e. the approaching main crack plus an undetermined number of slip zones on the interface) renders many of the existing numerical techniques impractical for this application.

*Accurate Representation of Near-Interface Crack Tip Fields:* When there remains but a narrow ligament separating an advancing fracture from a bonded bimaterial interface, the form of the singularity at the crack tip is known to deviate dramatically from the homogeneous case. As this is also reflected in the magnitude of the stress intensity factor, we can expect the interface to have pronounced effect on the fracture growth near bonded

fibers/inclusions. This class of problems is important both as a precursor to the onset of interfacial slip and to the limiting case of interfacial friction.

#### Surface Integral Method:

The effectiveness of the surface-integral method at modeling 3-D fractures in infinite regions is now well established.<sup>13,14</sup> It is based on representing a fracture as a distribution of force multipoles (or displacement discontinuities). Superimposing the differential effects of the constituent multipoles leads to the governing integral equation below:

$$s(\vec{x}) = \iint_{S_c} \bar{E} \gamma \delta(\vec{\zeta}) dA \quad (1)$$

where the scalar function  $s$  evaluated at  $x$  can represent any one of the displacement or stress components,  $\delta$  is the crack opening,  $E$  is a material constant relating crack opening to the equivalent multipole strength,  $S_c$  is the fracture surface, and  $\gamma$ , also known as the fundamental solution (or influence function), defines the effect on  $s$  of a multipole of unit strength. The influence functions can be found by differentiating the relevant point force solution in accordance with a Taylor series expansion (for details see Refs. 15,16). Thus we may note that the range of problems that can be solved by this method is limited by the availability of the point force solution.

The application of Eq. (1) requires that we first establish the magnitudes of the crack openings. An approach that works well is to generate a system of equations using boundary collocation, i.e., the known traction boundary conditions are enforced on the crack surface at as many points as there are unknown nodal values of crack opening. However the resulting equations are all singular at  $x=\zeta$  to the degree of being indeterminable. To bound the integrand, we subtract a singular function which by virtue of its being physically equivalent to a rigid-body translation, does not alter the equality. The following singular, but integrable, equation results:

$$t(\vec{x}) = \iint_{S_T} \bar{E} \gamma [\delta(\vec{\zeta}) - \delta(\vec{x})] dA \quad (2)$$

where  $t(x)$  refers to the tractions acting on the surface of the fracture and  $S_T$  spans the entire crack plane.

The advantages of the surface integral method may be summarized as follows. First, only the surface of the fracture has to be discretized; this considerably simplifies the process of remeshing the fracture as it grows. Second, the singularity at the crack tip does not require special treatment because its essential features are explicitly contained within the influence functions of the multipole. Third, accurate stress intensity factors can be obtained using coarse element meshes provided that a  $\rho^{1/2}$  variation of crack opening is assumed in the near-tip region, where  $\rho$  is the perpendicular distance from the crack front.

#### Surface Integral and Finite Element Hybrid Method:

With the existing library of influence functions being quite limited, the surface integral method cannot be directly applied to the problem of a fracture near an arbitrarily shaped region of material inhomogeneity. Thus to retain with such problems the advantages of a surface integral analysis, it has been combined with the finite element method using incremental superposition. The resulting hybrid method opens up the possibility of accounting for a wide range of volume effects, including material inhomogeneities<sup>13,17,18</sup>, thermal effects<sup>19</sup>, and plasticity.<sup>13,20</sup>

The following derivation of the governing hybrid equations considers the case, shown in Fig. 2, of a fracture which is fully embedded within a region of material inhomogeneity (referred to here as the subregion). It has been assumed that the only influence functions available for use are those for a multipole in an infinite, homogeneous region. It has further been assumed that the interface is sufficiently far away from the crack front so as not to either alter the form of the crack tip singularity or produce strong coupling at the interface, where the component methods will be joined.

A solution can be found by superimposing the results of the three models shown in Figure 2. Model I is an uncracked finite element model of the complete bounded domain. Model II is a surface integral model of the fracture in an infinite, homogeneous region. Since the results of Model II are not valid beyond the interface because of the mismatch in material properties, it is equivalently represented as a finite body being held in equilibrium

by tractions  $R^C$ . Model III is an uncracked finite element model of the subregion. It has been introduced to meet the requirement of displacement continuity at the interface. Since the component models of Fig. 2 individually satisfy equilibrium and strain compatibility within the limits of their respective formulations, all that remains to define the solution is to enforce both the prescribed boundary conditions and the traction/displacement continuity across  $\mathfrak{S}$ . This is accomplished through the application of corrective tractions and displacements.

Overall traction continuity across  $\mathfrak{S}$  is obtained by cancelling the tractions on the external boundaries of the two subregion models, i.e., models II and III. This is done by calculating a pair of nodal load vectors, representing the external traction distributions on each model, and applying the negative of both vectors to the interface nodes of model I. Thus the finite element equations for model I will have the standard form but with two additional load vectors on the right-hand side:

$$[K]\{U^{FE}\} = \{R\} - \{R^C\} - \{R^{SUB}\} \quad (3)$$

where  $[K]$  is the finite element stiffness matrix for model I,  $\{U^{FE}\}$  is the vector of unknown finite element nodal displacements, and  $\{R\}$  is the vector of prescribed nodal loads acting on model I. Defining the correction load vectors:  $\{R^C\}$  is a nodal force approximation of the surface integral tractions acting on  $\mathfrak{S}$  and thus may be reexpressed in terms of crack opening displacement;  $\{R^{SUB}\}$  refers to the nodal support reactions induced in model III by the imposition of nodal displacements  $\{U^{SUB}\}$  on the interface:

$$\{R^C\} = [G]\{\delta\}; \quad \{R^{SUB}\} = [K^{SUB}]\{U^{SUB}\} \quad (4)$$

where  $[K^{SUB}]$  is the finite element stiffness matrix for the subregion.

Displacement discontinuity across  $\mathfrak{S}$ , being already assured in model I, is enforced by requiring the interface nodes in model III to displace as the negative of displacements \* which are computed at the corresponding locations in model II:

$$\{U^{SUB}\} = -\{U^{SI}\} = -[L^{INT}]\{\delta\} \quad (5)$$

thus effectively cancelling the discontinuity in the displacement field introduced in model II when we truncated the surface integral domain at  $\mathfrak{S}$ .

The enforcement of traction boundary conditions at the crack surface is based on the surface integral equations of model II. Since the fracture has not been explicitly accounted for in either finite element model (i.e. I or III), these models will produce nonzero tractions,  $\{T^C\}$  and  $\{T^{SUB}\}$ , at locations coincident with the surface of the fracture. To cancel these extraneous tractions, they are reversed in sign and applied as additional boundary conditions in the surface integral formulation:

$$[C]\{\delta\} = \{T\} - \{T^C\} - \{T^{SUB}\} \quad (6)$$

The evaluation of  $\{T^C\}$  and  $\{T^{SUB}\}$  is based on the equations of those finite elements in models I and III, respectively, which would contain the fracture if it was to be explicitly modeled. Since the mesh topologies of finite element models I and III are identical for the subregion, it follows that:

$$\{T^C\} = [S]\{U^{FE}\}; \quad \{T^{SUB}\} = [S]\{U^{SUB}\} \quad (7)$$

where the same  $[S]$  applies to both  $\{T^C\}$  and  $\{T^{SUB}\}$ .

The final step in this derivation is to rewrite the above expressions as a system of equations in terms of designated primary variables  $U^{FE}$  and  $\delta$ . Two coupled systems of equations result when we substitute Eqs. (4) and (5) into (3), and Eqs. (7) and (5) into (6). When written in partitioned matrix form, they are expressed by:

$$\begin{bmatrix} K & G-K^{sub}L^{int} \\ S & C-SL^{int} \end{bmatrix} \begin{Bmatrix} U^{fe} \\ \delta \end{Bmatrix} = \begin{Bmatrix} R \\ T \end{Bmatrix} \quad (8)$$

Thermally-induced strains can be modeled with the SIFEH formulation. Linear, isotropic thermal effects are computed as correction load vectors and superimposed on the model presented above.<sup>21</sup> The resulting coupled system of equations takes the following form:

$$\begin{bmatrix} K & G-K^{sub}L^{int} \\ S & C-SL^{int} \end{bmatrix} \begin{Bmatrix} U^{fe} \\ \delta \end{Bmatrix} = \begin{Bmatrix} R+R^{th} \\ T-T^{th} \end{Bmatrix} \quad (9)$$

where  $\{R^{th}\}$  and  $\{T^{th}\}$  represent, respectively, the loading in the finite element model and on the crack surface due to thermal effects. Both correction load vectors can be computed using the surface integral and finite element formulations.

One of the key advantages of the hybrid method is that the surface integral model of the fracture can be set up independently of the finite element model of the surrounding domain. The implication of this for crack propagation analysis is that only the fracture surface has to be remeshed as the crack advances through the fixed finite element model. This feature has facilitated the development of a fully automatic remeshing algorithm, suitable for use on remote supercomputing facilities where interactive inspection of the crack mesh may not be available. The remeshing strategy is based on first representing the crack front as a parametric cubic spline and then dividing the fracture surface which it encloses into two domains: a leading edge region where tip elements assume a  $\rho^{1/2}$  variation of the crack opening, and an interior region where it suffices to employ low-order interpolation functions to capture the variation in crack opening. In the leading edge region where the shape and size of the tip element plays such a critical role in determining the accuracy of the stress intensity factors, heuristics are employed to construct the element geometries. The interior of the fracture is discretized by first dividing it into nearly convex subregions using a modified version of the algorithm proposed by Bykat<sup>22</sup> and then triangulating each subregion in succession using a method of geometric decomposition developed by Chae.<sup>23</sup>

#### DESCRIPTION OF EXPERIMENTAL INVESTIGATION:

The Resource Extraction Laboratory has developed a unique laboratory facility for the study of fracture growth near material inhomogeneity. Experimental simulation has supported and directed development of the SIFEH code. The apparatus used in this role are described in the following sections.

##### Crack Interaction Apparatus (CIA):

The model system is composed of 1.8 cm diameter glass rods embedded in large cement cylinders. The specimens are tested in the specially designed crack interaction apparatus (CIA) shown schematically in Figure 3. The CIA allows independent control of

the axial and radial stresses exerted on the specimen during testing. By internally pressurizing a precrack cast into the cement, a quasi-static fracture is propagated in the specimens, perpendicular to one or more rods (fibers). Brief deviations from a hydrostatic stress boundary condition leave small stairstep markings on the fracture surface, thereby recording the history of an advancing crack as it approaches and bows around the glass inclusions. Successive stages in crack development can be observed on each of the resulting halves of a ruptured specimen. By coating the glass rods prior to casting, the friction coefficients may be controlled and its impact assessed. Figure 4 shows representative crack growth patterns for high and low friction interfaces.

Interfacial properties for coated glass rods cast in cement are determined experimentally with push-out tests. Glass rods (fibers) are driven from the surrounding cylindrical specimens (in a state of hydrostatic compression) using an Instron test apparatus. Load-displacement histories are then evaluated to determine cohesion and frictional slip properties.

#### Interfacial Separation Experiment (ISE):

ISE simulates the growth of the slip zone on a planar interface normal to a pressurized crack. The apparatus uses transparent materials with variable crack geometries and interfacial friction coefficients to visually observe interfacial slip between the media. (see Figures 5,6) Computer mapping of measured interface displacements determines the shape and size of the evolving zone.

#### APPLICATIONS:

##### Crack Growth Near a Planar Bimaterial Interface:

The growth of a pressurized fracture toward a bonded bimaterial interface was modeled using the previously described surface integral method. The near-interface crack tip fields are accurately captured by employing the influence functions for a dipole near a planar bimaterial interface (see Figures 7,8 and Tables 1,2). These influence functions explicitly account for the presence of the interface so that only the surface of the fracture has to be discretized. To obtain the fracture shape shown in Figure 9, points along the

initially circular crack front were incrementally advanced in proportion to the local values of  $(K_I - K_{IC})$  with  $K_{IC}$  representing fracture toughness.

#### Fracture Intersecting Multiple Bimaterial Interfaces:

The surface integral formulation could not be directly applied to model a fracture intersecting two bimaterial interfaces because the corresponding influence functions were not available. Superposition of results derived with sets of bimaterial influence functions and application of appropriate correction loads allows accurate modeling of near-interface fracture behavior. Results obtained for fractures near two planar bimaterial interfaces are presented in Figures 10-14 and Table 3.

#### Interaction of Multiple 3-D Mixed Mode Fractures:

Toughening brittle materials with second phase brittle fibers involving tailoring microstructures, material properties, fiber spacing, interfaces, etc. to create an environment that favors the growth of smaller flaws over the continued growth of some dominant propagating flaw. Assessing the resulting pseudo-ductility involves the interaction of multiple fractures. There are relatively few solutions in the literature for mixed-mode interaction of numerous cracks. The surface integral method accurately replicates these existing solutions, but is not limited to simple geometries or loading. Figure 15 illustrates the variation in the stress intensity factor with distance between two parallel cracks. Results correlate well with the solutions in Ref. 26. Similar results are obtained for two coplanar cracks as shown in Figure 16.

#### Surface Cracks:

The SIFEH method has proven useful for modeling surface cracks in bounded domains. The bimaterial influence functions are combined using superposition as shown in Figure 17. The case of a semi-circular surface crack in a finite-thickness plate under uniform tension was used to test the approach. This geometry was investigated by Raju and Newman<sup>27</sup> using finite element methods and has been verified by subsequent studies. With minor refinement of the finite element mesh in the region of the surface flaw, the SIFEH method accurately represented the stress intensity factors along the crack front as shown in Figures 18 and 19. Similar results were obtained for the case of semi-elliptical

### Evolution of Frictionally Constrained Interfacial Slip:

The interfacial decohesion and slipping at the periphery of a dominant flaw (fracture) as it first encounters a fiber is the critical episode for determining subsequent crack deflection, blunting, bowing, and/or reinitiation across the fiber-matrix interface. The frictional tractions at the sliding interface provide the key energy dissipating mechanism for inhibiting fracture propagation. The fully 3-D determination of the extent of the sliding zone and the nonlinear coupling between it and the impinging crack presents a formidable challenge that has not previously been accomplished. The following coupled integral equations explicitly demonstrate the role of the coefficient of friction ( $\mu$ ), the residual stresses across the interface ( $\sigma_{ni}$ ), and the applied tractions ( $\sigma$ ) in determining the extent of the slip zone ( $S_c$ ) and the propensity for the main crack growth:

$$\text{Main Crack: } \sigma(\vec{x}) = \iint_{S_c} \gamma \delta(\vec{\zeta}) dA + \iint_{S_S} \gamma \delta(\vec{\zeta}) dA \quad (10)$$

$$\text{Sliding Zone: } \sigma_n(\vec{x}) - \sigma_{ni}(\vec{x}) = \iint_{S_S} \gamma_n \delta(\vec{\zeta}) dA + \iint_{S_c} \gamma_n \delta(\vec{\zeta}) dA$$

$$\tau_n(\vec{x}) - \mu \sigma_n(\vec{x}) = \iint_{S_S} \gamma_t \delta(\vec{\zeta}) dA + \iint_{S_c} \gamma_t \delta(\vec{\zeta}) dA$$

Figure 5 shows the characteristic zones for the onset of slip near a circular pressurized crack for a specific set of parameters.

## CONCLUSIONS

Three-dimensional computational and experimental investigations have resulted in novel tools for the investigation into the toughening mechanisms due to incorporation of brittle fibers in brittle matrices. Application of the surface integral and finite element hybrid (SIFEH) method to a wide variety of fracture geometries in bimaterial media have shown the technique to be a flexible and efficient tool. Incorporation of thermally-induced strains and interfacial decohesion/frictional slip have further enhanced the capabilities of the method. When combined with experimental studies, the method developed will help brittle composite manufacturers tailor the material properties to suit material demands.

References:

- <sup>1</sup>Ming-Yuan He and J.w. Hutchinson, "Crack Deflection at an Interface Between Dissimilar Elastic Materials," *Int. J. Solids Struct.*, **25**[1] 1053-1067 (1989).
- <sup>2</sup>K.Y. Lam and M.P. Cleary, "Slippage and Re-Initiation of (Hydraulic) Fractures at Frictional Interfaces," *Int. J. Numer. Anal. Meth. Geomech.*, **8**, 589-604 (1989).
- <sup>3</sup>F.Erdogan and Askogan, "Bonded Half Planes Containing an Arbitrarily Oriented Crack," *Int. J. Solids Struct.*, **10**, 569-585 (1974).
- <sup>4</sup>M.K. Kanninen, E.F. Rybicki, and W.I. Griffith, "Preliminary Development of a Fundamental Analysis Model for Crack Growth in a Fiber Reinforced Composite Material"; pp.53-69 in *Composite Materials: Testing and Design. ASTM 617*, American Society for Testing and Materials, 1976.
- <sup>5</sup>F. Erdogan and G.D. Gupta, "The Inclusion Problem with a Crack Crossing the Boundary," *Int. J. Fract.*, **11**[1] 13-27 (1975).
- <sup>6</sup>B. Budiansky, J.W. Hutchinson, and A.G. Evans, "Matrix Fracture in Fiber-Reinforced Ceramics," *J. Mech. Phys. Solids*, **34**[2] 167-189 (1986).
- <sup>7</sup>B. Budiansky and John Amazigo, "Toughening by Aligned, Frictionally Constrained Fibers," Harvard University Report MECH-119 (Mar., 1988).
- <sup>8</sup>D.B. Marshall, B.M. Cox, and A.G. Evans, "The Mechanics of Matrix Cracking in Brittle-Matrix Fiber Composites," *Acta Metall.*, **33**[11] 2013-2021 (1985).
- <sup>9</sup>L.S. Sigl and A.G. Evans, "Effects of Residual Stress and Frictional Sliding on Cracking and Pull-Out in Brittle Matrix Composites," *Mech. Mater.*, **8**, 1-12 (1989).
- <sup>10</sup>J.W. Hutchinson and H.M. Jensen, "Models of Fiber Debonding and Pullout in Brittle Composites with Friction," Harvard University Report MECH-157 (Feb., 1990).
- <sup>11</sup>A.G. Evans, "The Strength of Brittle Materials Containing Second Phase Dispersions," *Phil. Mag.*, **26**, 1327-1344 (1972).
- <sup>12</sup>Nabil Fares, "Crack Fronts Trapped by Arrays of Obstacles: Numerical Solutions Based on Surface Integral Representation," Harvard University Report MECH-136 (Nov., 1988).
- <sup>13</sup>W.D. Keat, B.S. Annigeri, and M.P. Cleary, "Surface Integral and Finite Element Hybrid Method for Two and Three-Dimensional Fracture Mechanics Analysis," *Int. J. Fract.*, **36**[1] 35-53 (1988).
- <sup>14</sup>W.D. Keat, "Surface Integral and Finite Element Hybrid Method for the Analysis of Three-Dimensional Fractures," Ph.D. Thesis in the Department of Mechanical Engineering, M.I.T., April, 1989.
- <sup>15</sup>M.P. Cleary, "Fundamental Solutions for a Fluid-Saturated Porous Solid," *Int. J. Solid Struct.*, **13**, 785-806 (1977).

<sup>16</sup>B.H.G. Brady, "A boundary Element Method for Three-Dimensional Elastic Analysis of Tabular Orebody Extraction," *19th U.S. Rock Mechanics Symposium*, 431-439 (1978).

<sup>17</sup>B.S. Annigeri, W.D. Keat, and M.P. Cleary, "Fracture Mechanics Research Using the Surface Integral and Finite Element Hybrid Method"; Proceedings of First Joint Japan/U.S. Symposium on Boundary Element Methods. University of Tokyo, Oct., 1988. Pergamon Press, New York.

<sup>18</sup>W.D. Keat and M.P. Cleary, "Analysis of 3-D Near-Interface Fractures in Bounded Heterogeneous Domains Using the Surface Integral and Finite Element Hybrid Method"; pp. 343-352 in Proceedings of International Symposium on Boundary Element Methods. United Technologies Research Center, Oct., 1989. Springer-Verlag.

<sup>19</sup>B.S. Annigeri, "Thermoelastic Fracture Analysis using the Surface Integral and Finite Element Hybrid Method"; presented at the ICES-88 Conference, Atlanta, Georgia, 1988.

<sup>20</sup>B.S. Annigeri, "Surface Integral Finite Element Hybrid Method for Localized Problems in Continuum Mechanics," Sc.D. Thesis in the Department of Mechanical Engineering, M.I.T., April, 1984.

<sup>21</sup>R.J. Bsaibes, "Analysis of Three-Dimensional Fractures Subject to Thermal Loading," B.S. Thesis in the Department of Mechanical Engineering, M.I.T., June, 1991.

<sup>22</sup>A. Bykat, "Automatic Generation of Triangular Grid: I-Subdivision of a General Polygon into Convex Subregions, II-Triangulation of Convex Polygons," *Int. J. for Numerical Methods in Engineering*, **10**, 1329-1342 (1976).

<sup>23</sup>S.W. Chae, "On the Automatic Generation of Near-Optimal Meshes for Three-Dimensional Linear Elastic Analysis," Ph.D. Thesis in the Department of Mechanical Engineering, M.I.T., 1988.

<sup>24</sup>Rongved, "Force Interior to One of Two Joined Semi-Infinite Solids"; pp. 1-13 in Proceedings of Second Midwestern Conf. on Solid Mech., 1955.

<sup>25</sup>M.P. Cleary, "Primary Factors Governing Hydraulic Fractures in Heterogeneous Stratified Porous Formations"; presented at Energy and Petroleum Conference, Houston, November, 1978, ASME Paper No. 78-Pet-47, 1978.

<sup>26</sup>Murakami, Stress Intensity Factors Handbook, Vol. 2. Pergamon Press, New York, 1987.

<sup>27</sup>I.S. Raju and J.C. Newman, "Stress-intensity factors for a wide range of semi-elliptical surface cracks in finite thickness plates", *Engin. Fract. Mech.*, **11**, 817-829 (1979).

<sup>28</sup>T.S. Cook and F. Erdogan, "Stresses in bonded materials with a crack perpendicular to the interface", *Int. J. Engin. Sci.*, **10**, 677-697 (1972).

<sup>29</sup>F. Erdogan and V. Biricikoglu, "Two bonded half planes with a crack going through the interface", *Int. J. Engin. Sci.*, **11**, 745-766 (1973).

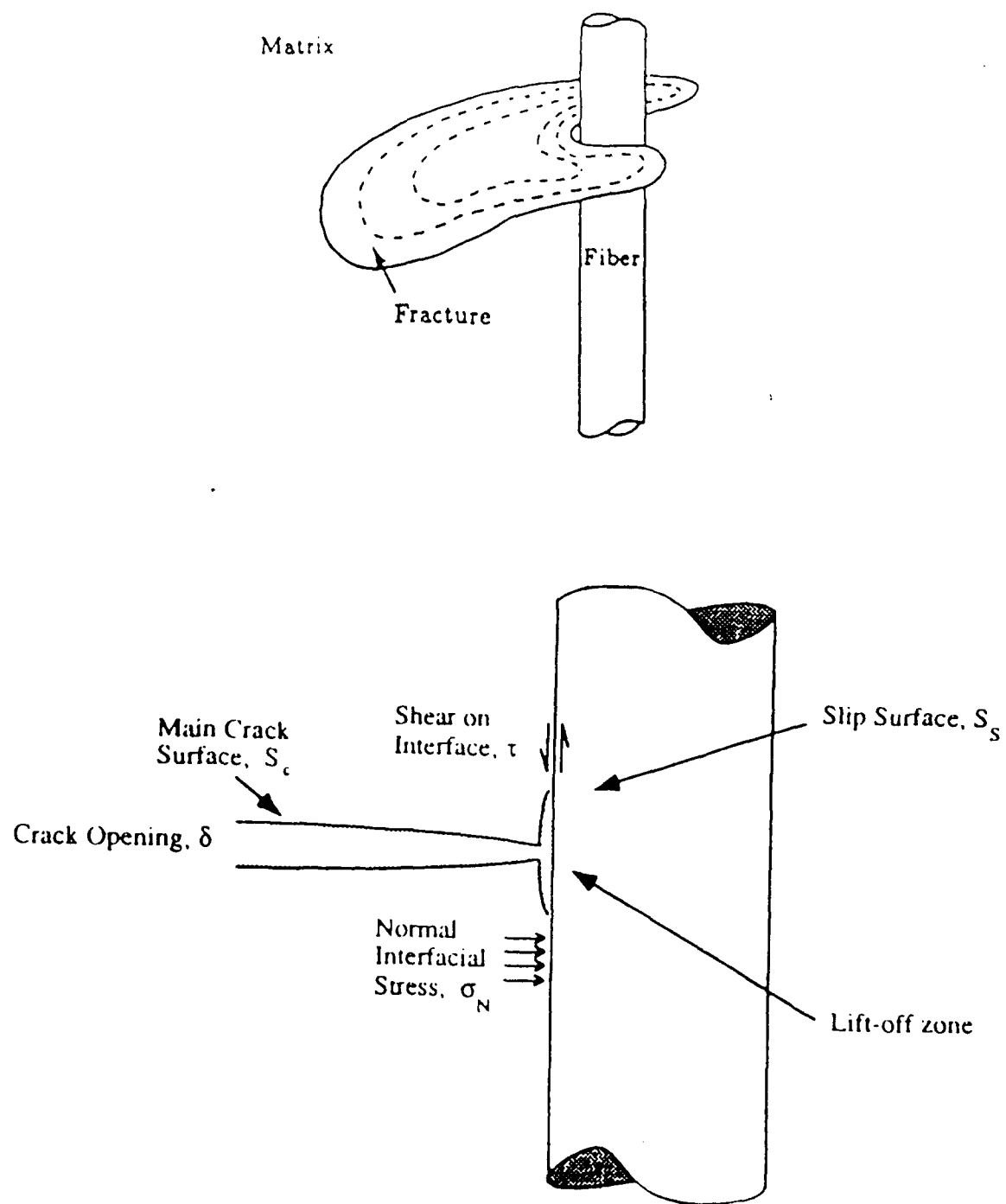


Figure 1. Representations of a crack periphery encountering a fiber.

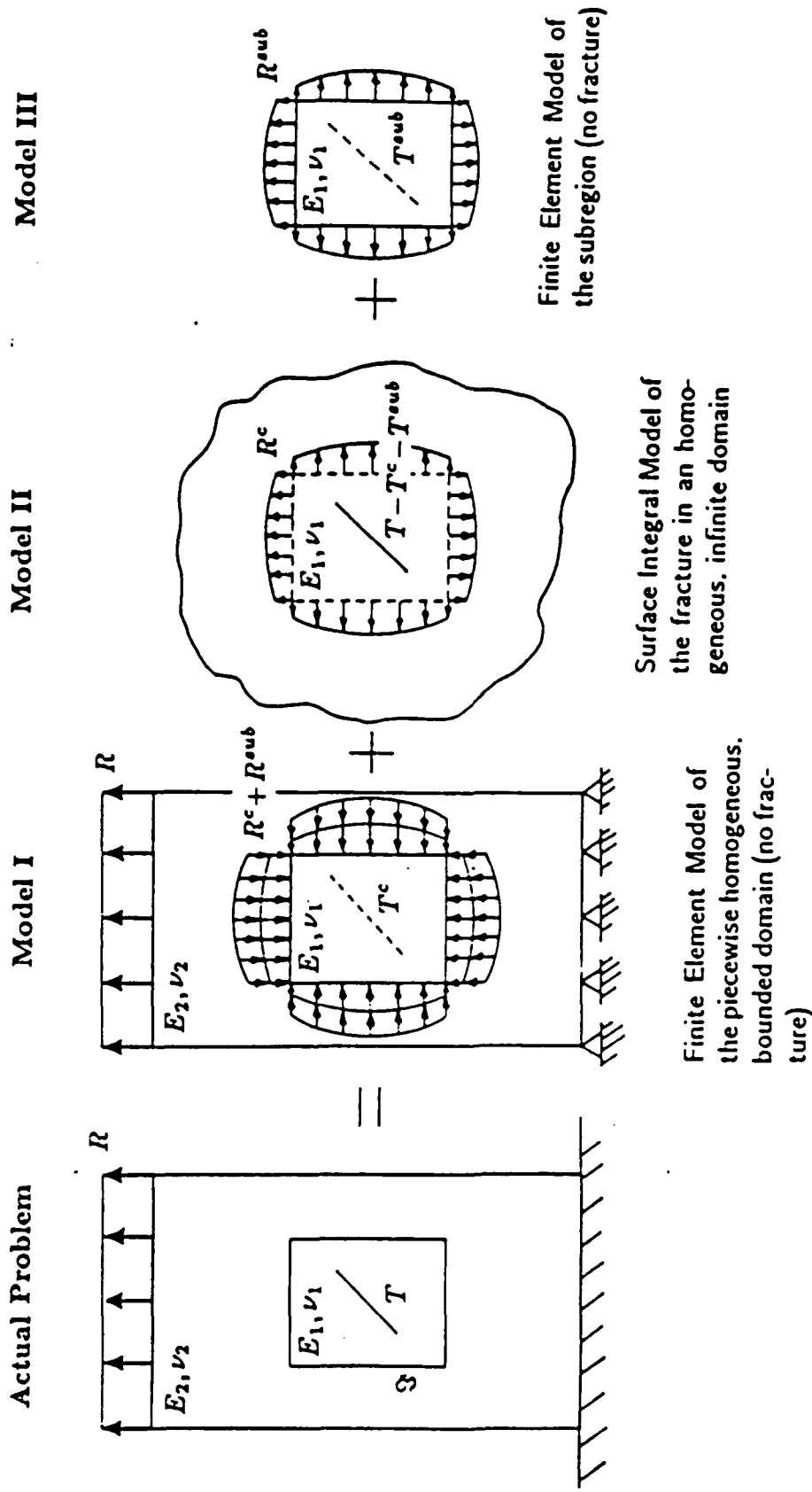


Figure 2. Component models used with subregioning.

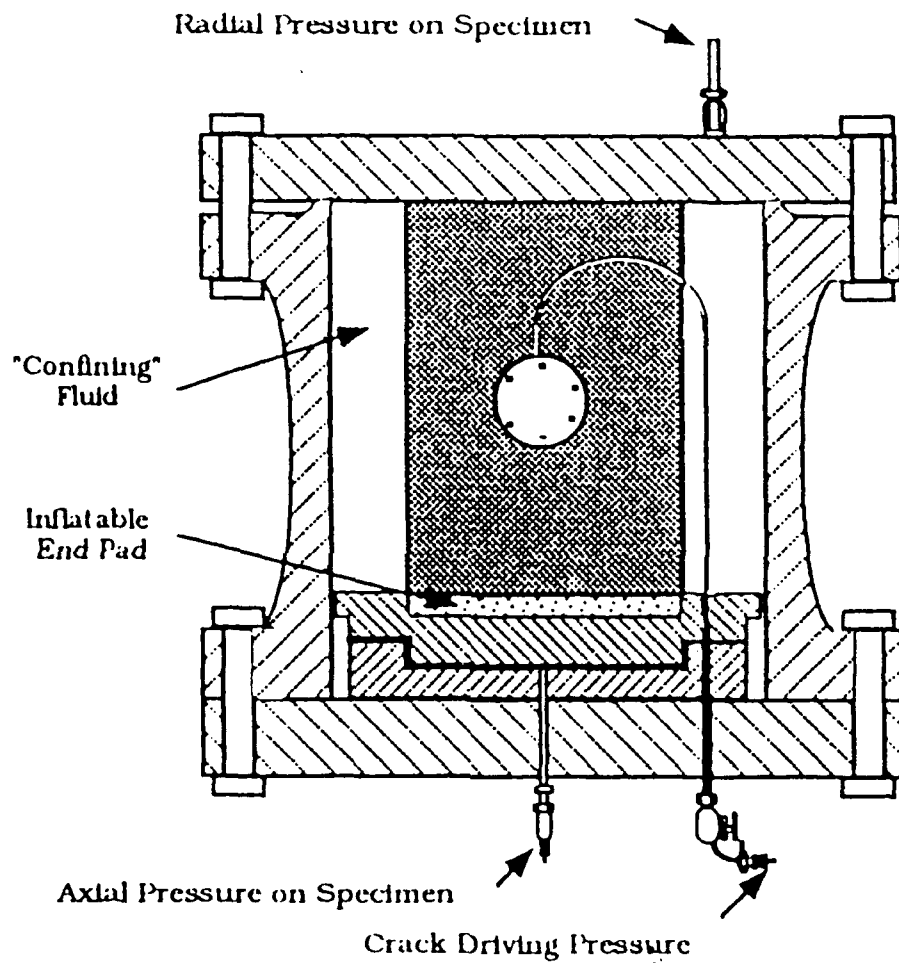


Figure 3. Hydraulic fracturing test apparatus used to grow quasi-static cracks toward cylindrical inclusions. Independent control of the axial and radial pressures permits periodic marking of the crack front.

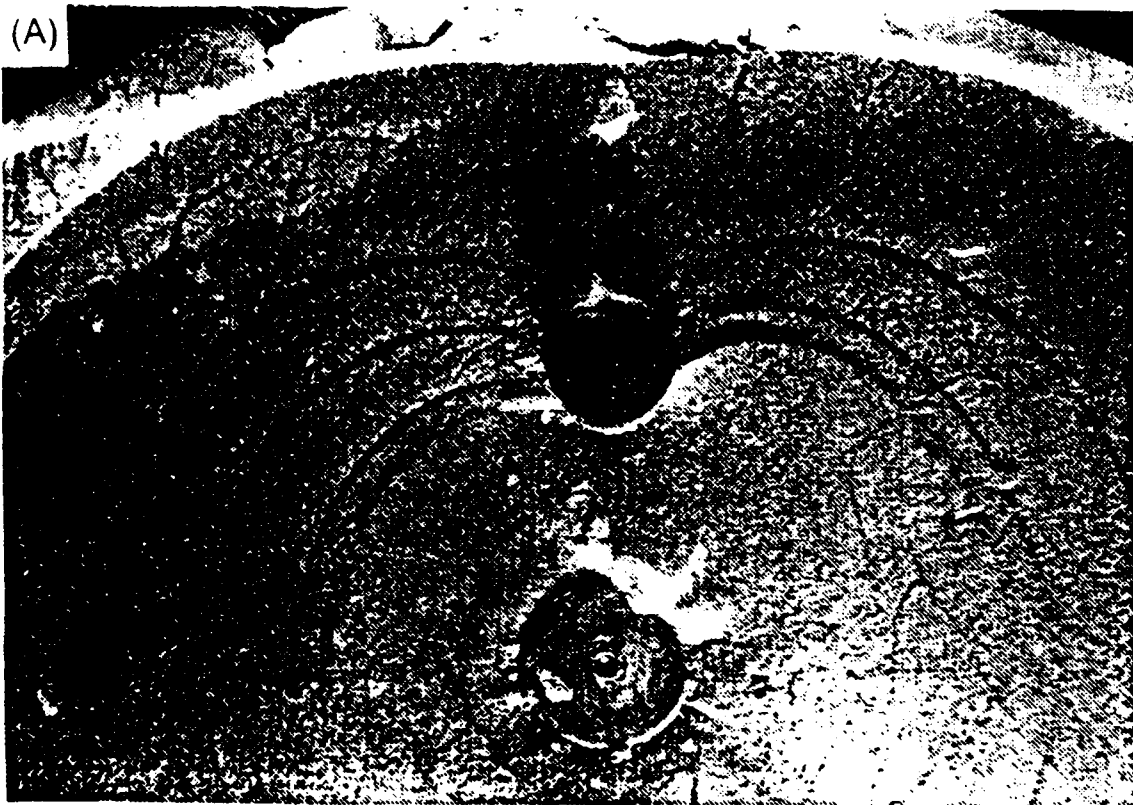


Figure 4. Representative photographs showing the local influence of a brittle inclusion on fracture propagation. The two contrast the growth patterns around a brittle fiber for a "strong" (a) and a "weak" (b) interface.

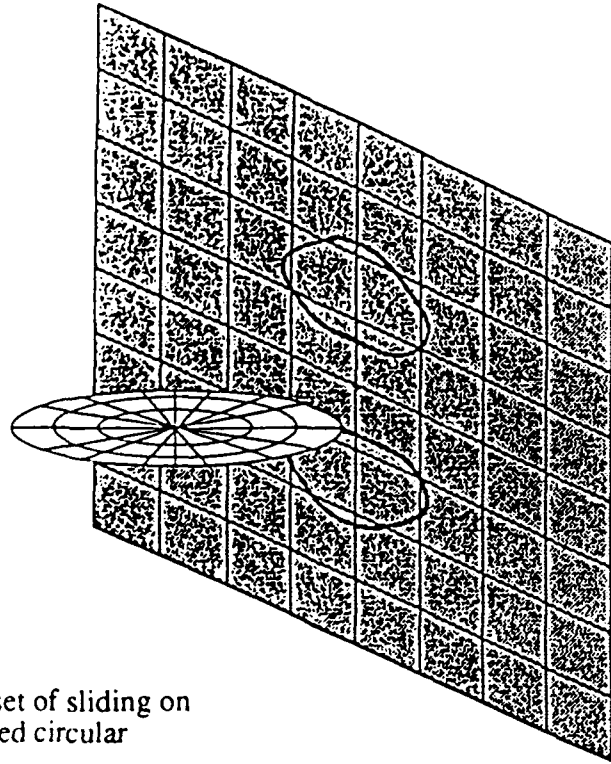


Figure 5. Schematic showing the onset of sliding on a planar interface ahead of a pressurized circular crack.

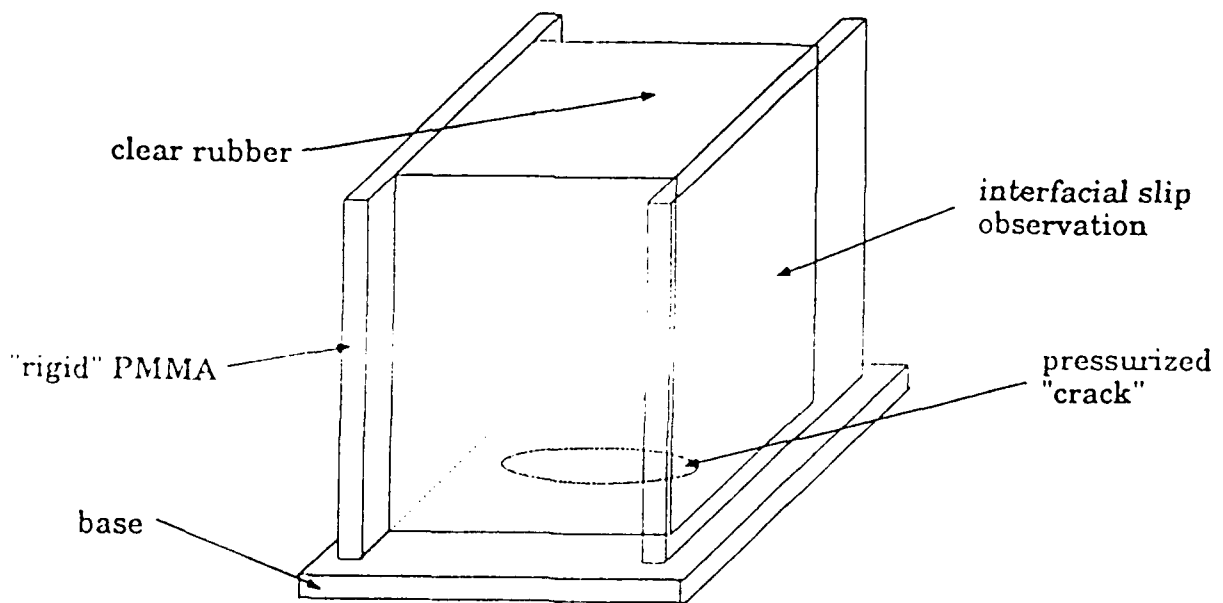


Figure 6. Schematic of ISE apparatus for direct observation of interfacial slip near a material discontinuity (crack).

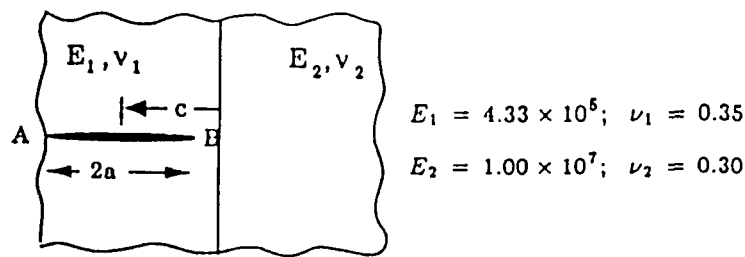


Figure 7. Fracture (under plane strain conditions) approaching a single planar bimaterial interface. See Table 1 for results.

$c/a$	$\left(\frac{K_I}{\sigma\sqrt{\pi a}}\right)_A$	(% Deviation) <sub>A</sub>	$\left(\frac{K_I}{\sigma\sqrt{\pi a}}\right)_B$	(% Deviation) <sub>B</sub>
2.0	0.9682	0.686	0.9416	0.717
1.25	0.9202	0.404	0.7887	0.625
1.15	0.9078	0.298	0.7250	1.003
1.10	0.9010	0.278	0.6787	1.693
1.00	0.8841	0.159	0.5221*	—

Table 1. Comparison of Cook and Erdogan's<sup>28</sup> plane strain solution with the 3-D surface integral results.

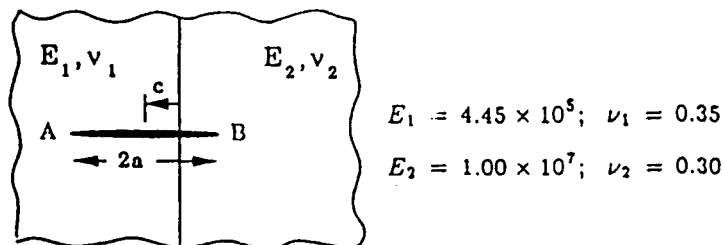


Figure 8. Fracture (under plane strain conditions) intersecting a planar bimaterial interface. See Table 2 for results.

$c/a$	$\left(\frac{K_I}{P_1\sqrt{\pi a}}\right)_A$	(% Deviation) <sub>A</sub>	$\left(\frac{K_I}{P_2\sqrt{\pi a}}\right)_B$	(% Deviation) <sub>B</sub>
1.0	0.8840	0.147	—	—
.75	0.8734	0.000	0.5597	-5.245
.50	0.9124	-0.642	0.7916	-1.395
.25	0.9984	-1.723	0.9524	-1.008
0.0	1.144	-2.97	1.083	-0.923
-.25	1.378	-4.149	1.194	-0.870
-.50	1.774	-5.203	1.287	-0.946
-.75	2.621	-5.304	1.364	-1.132
-1.0	—	—	1.360	0.354

Table 2. Comparison of Erdogan and Biricikoglu's<sup>29</sup> plane strain solution with the 3-D surface integral results.

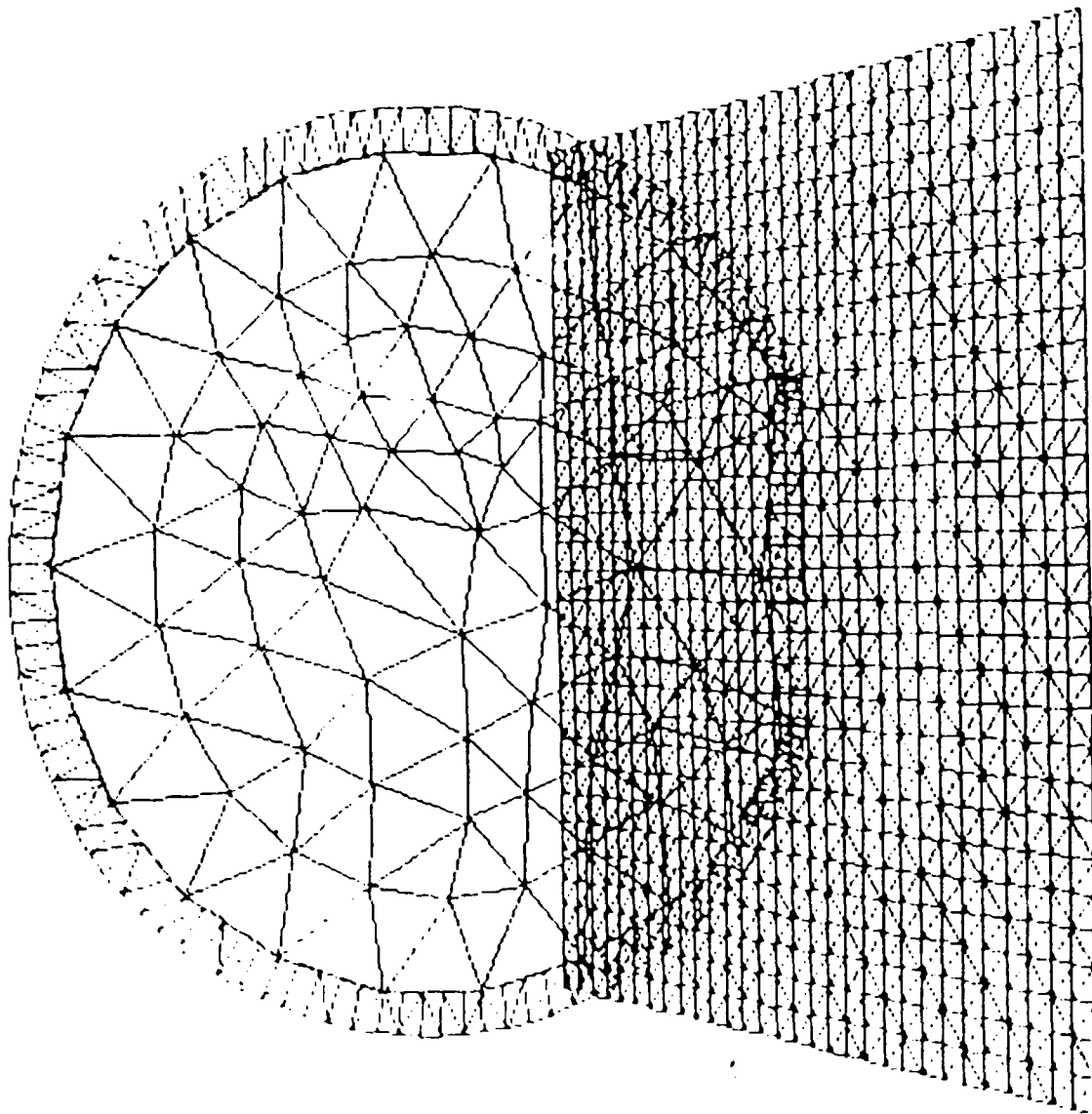


Figure 9. Snapshot from an animation showing the blunting of a fracture as it reaches a planar bimaterial interface. The fracture lies in the softer medium.

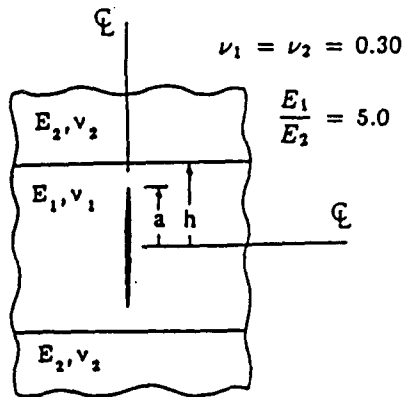


Figure 10. Fracture (under plane strain conditions) approaching two planar bimaterial interface. See Table 3 for results.

a/h	$\frac{K_I}{\sigma\sqrt{\pi a}}$	% Deviation
0.3	1.040	0.970
0.6	1.156	0.522
0.9	1.611	2.611

Table 3. Comparison of Hilton and Sih's plane strain solution with the 3-D hybrid results.

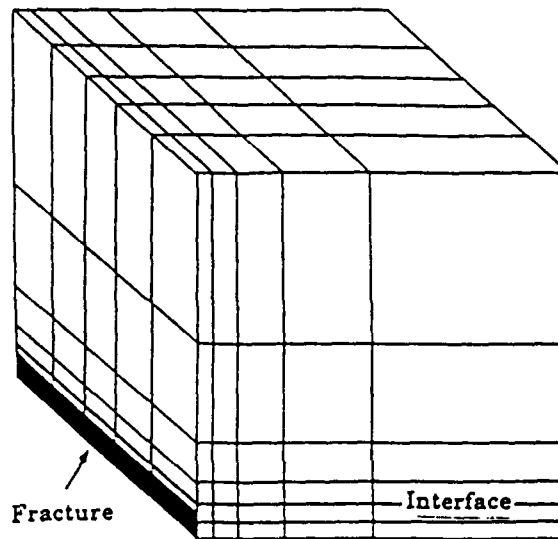


Figure 11. 1/8 symmetric hybrid model used with the double interface problem.

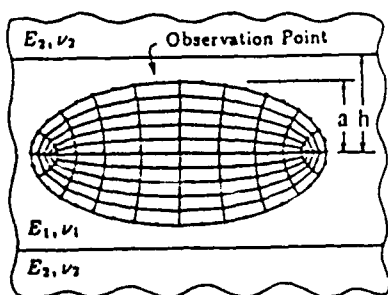


Figure 12. Elliptical fracture approaching two planar bimaterial interfaces. The fracture has been represented by its surface integral discretization.

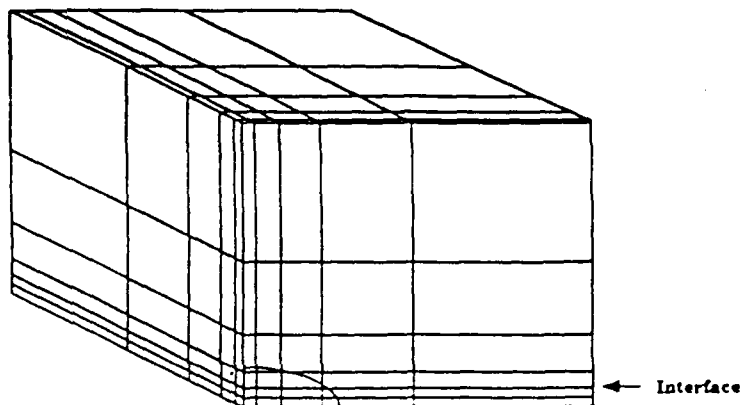


Figure 13. 1/8 symmetric model of the elliptical fracture in a tri-layered domain.

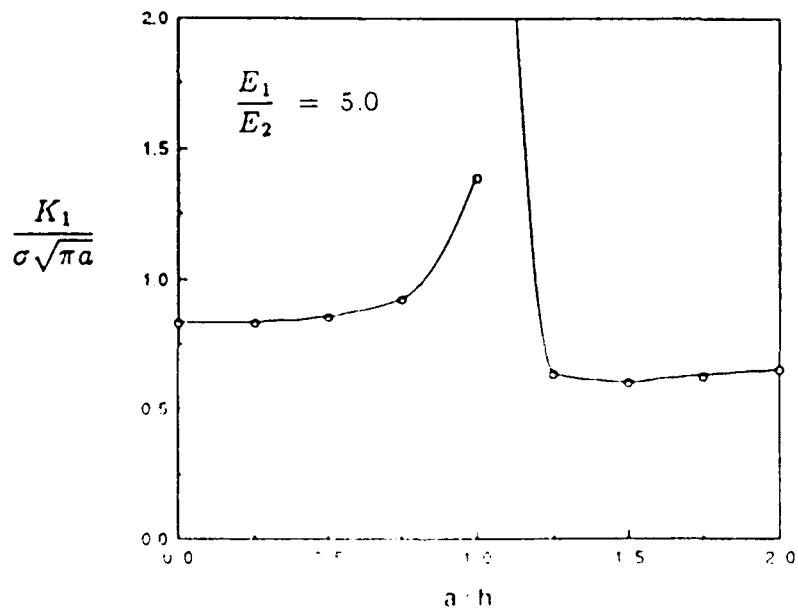
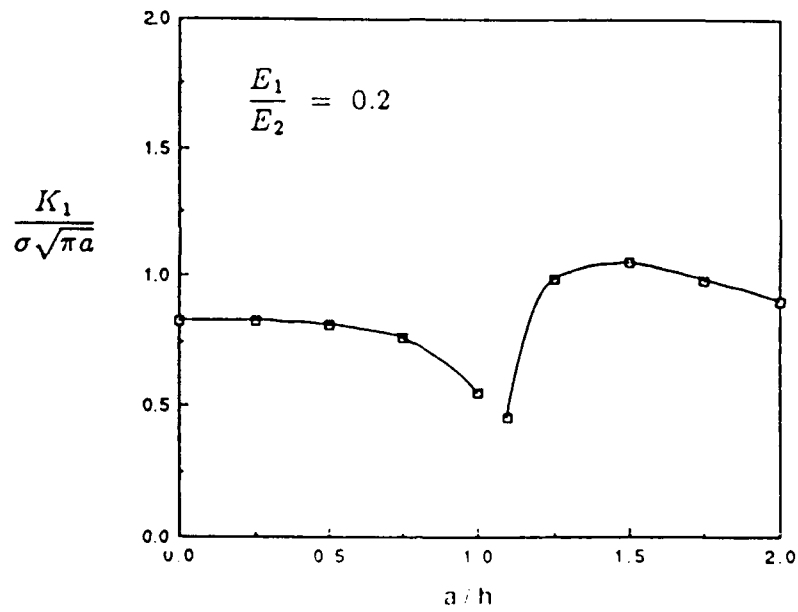


Figure 14. Dependence of  $K_1$  on the value of  $a/h$  for a 3-D elliptical fracture in a tri-layered domain. Results for two different ratios of the elastic moduli are presented. Values of  $K_1$  were recorded at the observation point indicated in Figure 12.

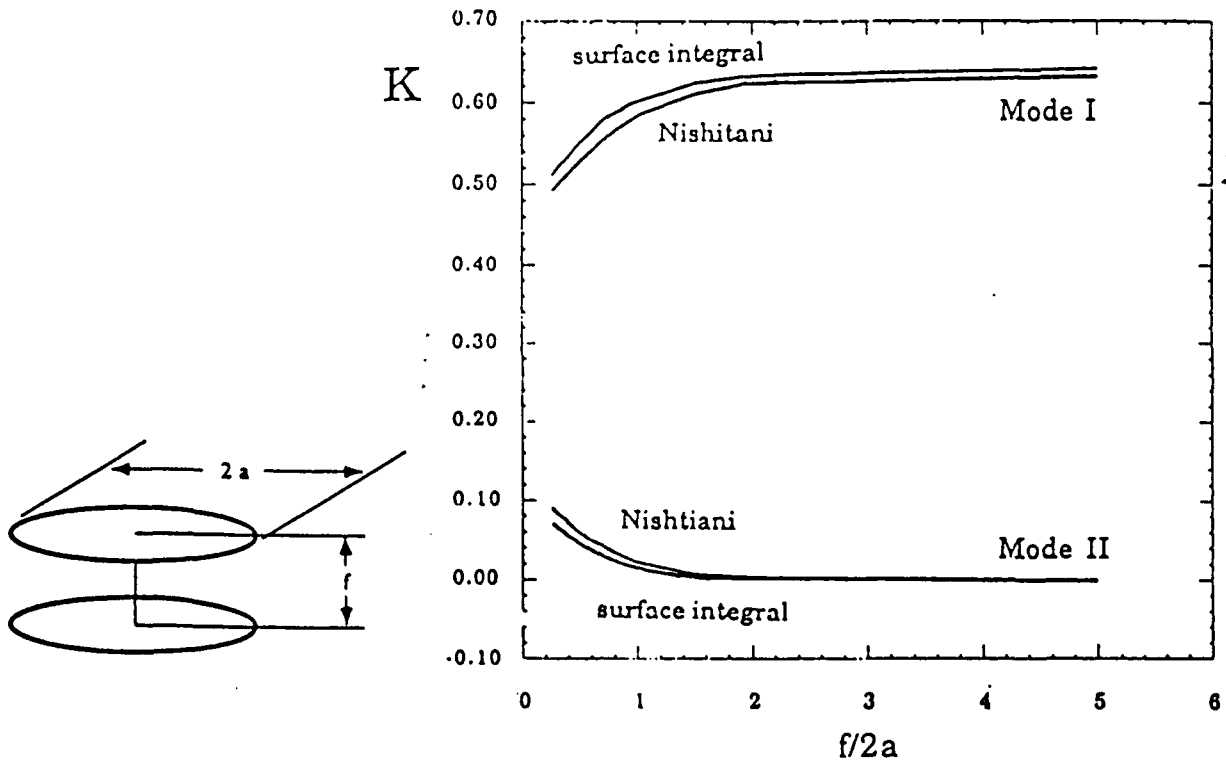


Figure 15. Variation of Mode I and Mode II stress intensity factors with distance between parallel circular cracks.

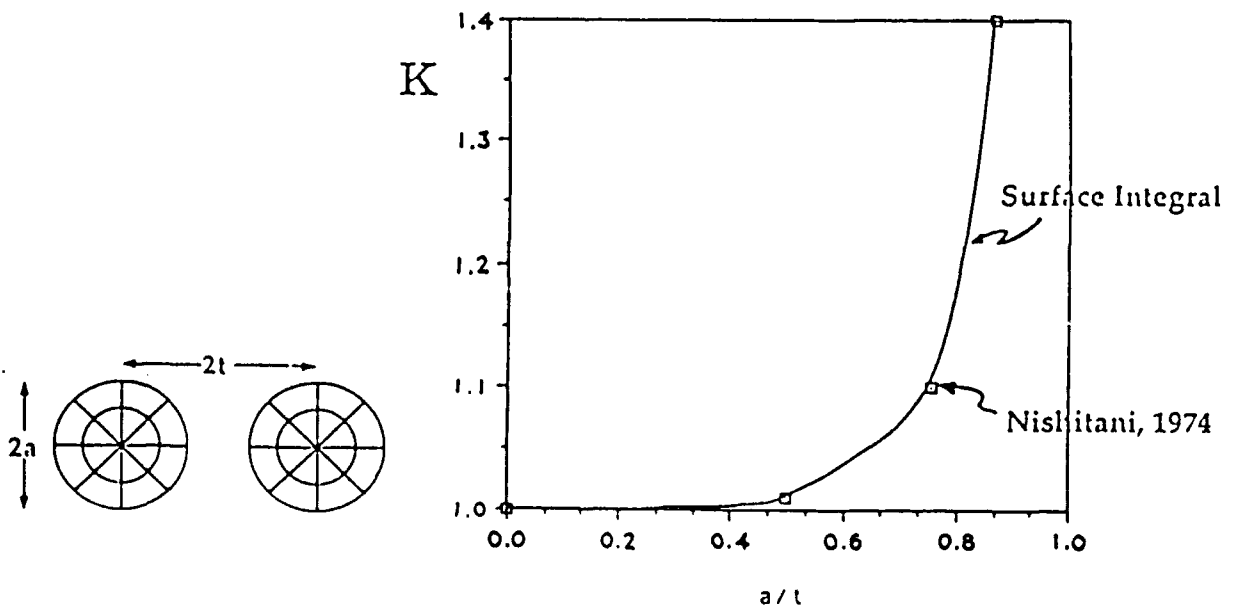
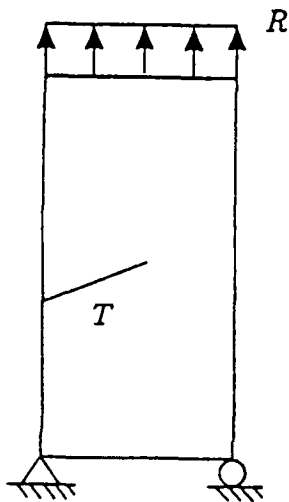


Figure 16. Variation in maximum stress intensity factor with distance between coplanar cracks.

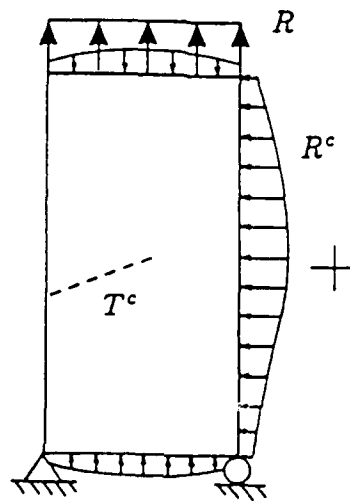
Actual Problem

Model I

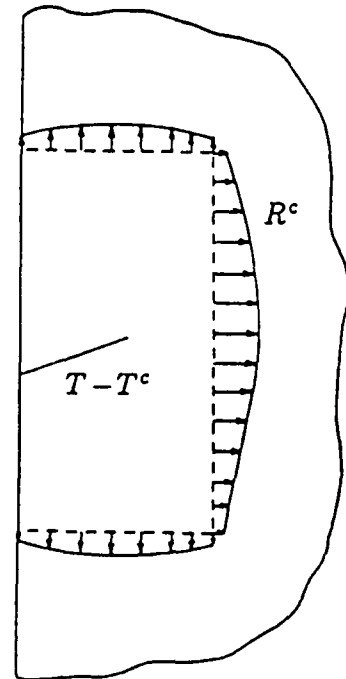
Model II



=



+



Finite Element Model of the bounded domain (no fracture)

Surface Integral Model of the fracture in a semi-infinite domain

Figure 17. Component geometries used with the hybrid method to model a surface crack in a bounded domain.

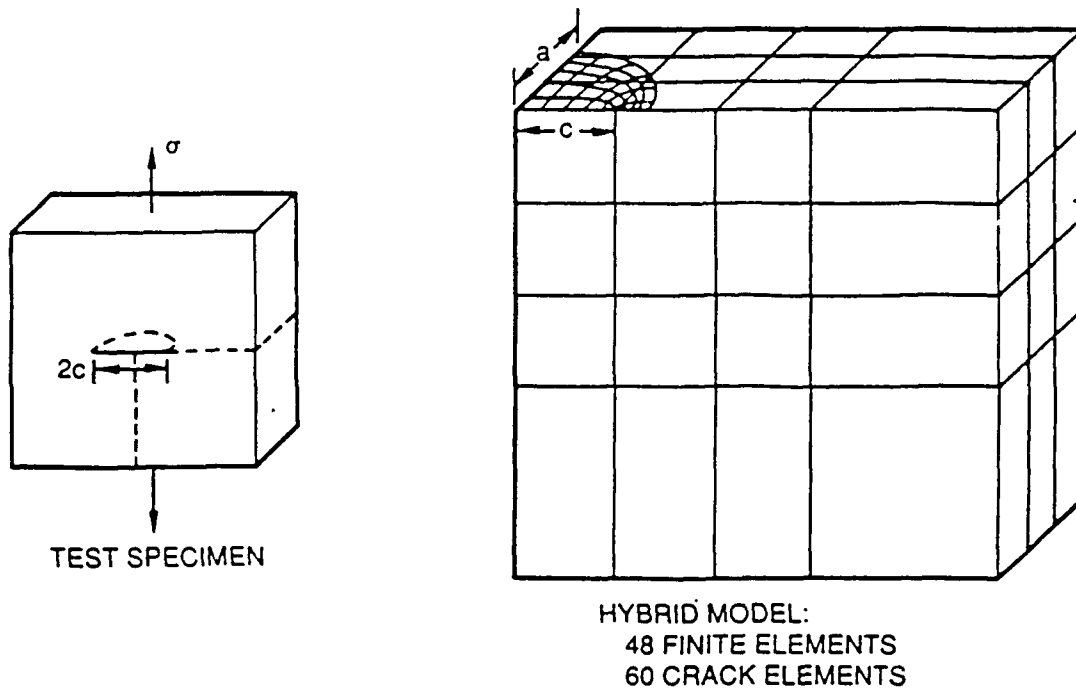


Figure 18. Specimen geometry and corresponding hybrid model used in fatigue crack growth study.

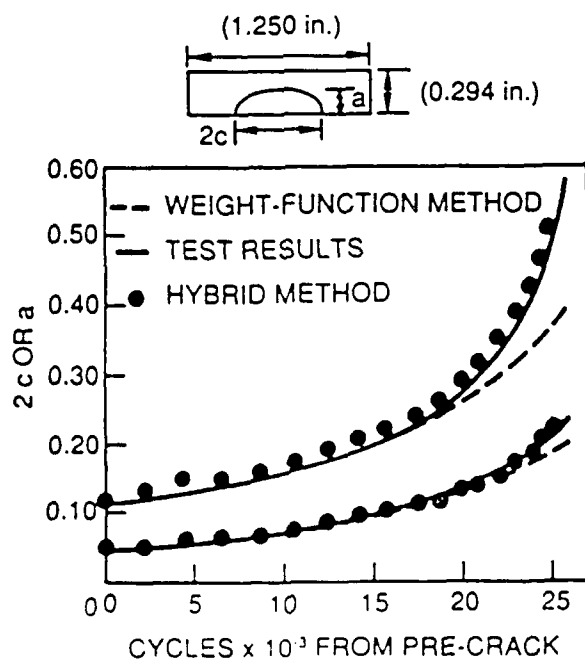


Figure 19. Comparison of SAFE and experimental results for growth of a surface crack in a thick plate.